A theoretical study of *cis–trans* isomerisation in H-ZSM5: probing the impact of cluster size and zeolite framework on energetics and structure

Duangkamol Gleeson

Abstract In this study the results from a series of calculations are reported that probe the influence of the QM cluster size and the extended framework treatment in ONIOM calculations. This is done by comparing the differences in the structures and energetics obtained during simulations of *cis–trans* isomerisation of butene in H-ZSM-5 at varying level of accuracy. Seven different models have been employed; 3T, 5T and 10T DFT cluster models, and to more effectively encode the extended framework of ZSM-5; 3T:46T, 5T:46T, 10T:46T DFT:MM ONIOM models, and a 46T DFT cluster model. The results show that irrespective of the exact QM cluster size, relatively small gasphase clusters show clear limitations due to the neglect of the extended framework. In particular, the structural and electronic implications of using the different zeolite models have been rigorously assessed using the multivariate statistical method principal components analysis (PCA).

Introduction

Zeolites are microporous molecular sieves which typically consist of interconnected tetrahedra of silicon and oxygen

D. Gleeson (✉)
Chemistry Department, Faculty of Science, King Mongkut's Institute of Technology Ladkrabang, Bangkok 10520, Thailand
e-mail: ktduangk@kmitl.ac.th

atoms arranged into a complex 3-dimensional arrangement of inter-connecting channels and cavities [1] (Fig. 1). This gives rise to the unique catalytic characteristics of the zeolites, a function of their Brønsted acidity, their local pore structure and the long-range stabilisation provided by the zeolite framework.

A considerable amount of scientific resource has been devoted to the research of zeolites as replacements for traditional media employed as catalysts in the transformation hydrocarbons. In particular, quantum mechanical (QM) simulations have been extensively employed to study concepts in zeolite catalysis, offering a unique way to rationalise experimental results. Simulations of zeolites have ranged from the use of small QM clusters (3T [2, 3] & 5T [4, 5]), large ring clusters [4–6], or more complete representations of the zeolite lattice using ONIOM [4, 7–9], QM/MM [10, 11] or alternate embedded/periodic methods [9, 12–16]. These references represent a very small sample of those available in the literature and have been highlighted by the author due to the direct relevance to this study.

Early simulations of zeolites were restricted to small QM clusters treated at low levels of theory, but with the advent of cheap and ever quicker processors, larger, more accurate simulations have become common, exposing the limitations in many previous simulations. Rozanska et al. [14] for example report that small QM clusters and DFT periodic models display the same trends with respect to the activation energies for alkylation of benzene in mordenite, however the latter energies are significantly larger by ∼15 kcal/mol. Jansang et al. [8] report that 3T and 10T cluster models significantly underpredict the adsorption energies of benzene in mordenite compared to 120T ONIOM and periodic simulations. Additionally, Solans-Monfort et al. [9] report that small cluster model simulations of NH_3 adsorption in
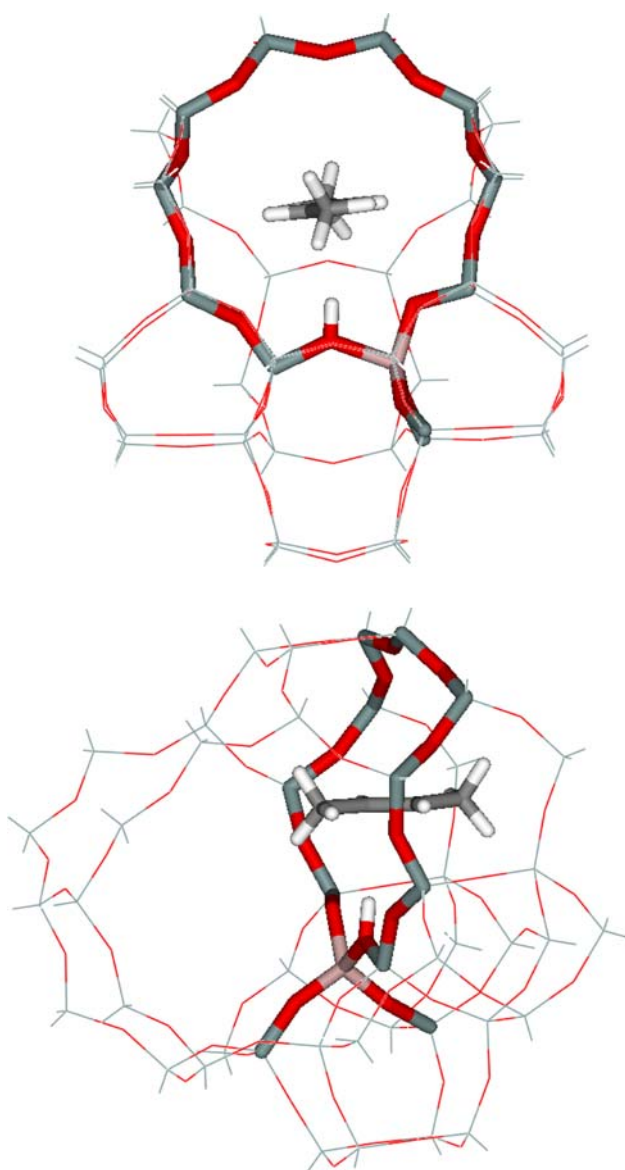
Fig. 1 An illustration of the 46T ZSM-5 model used here. The main 10T ring of ZSM-5 and chemisorbed *trans*-butene molecule are represented using a stick representation

mordenite are unable to reproduce the structure or adsorption energy when compared to ONIOM or periodic DFT simulation. Nonetheless, while there are clear limitations of small clusters, Boronat et al. [5] report that the cluster approach can realise comparable energies to the periodic approach if of a sufficient size such that the model in question can account for the key steric, electronic and van der Waals effects of the zeolite framework. More recently Tuma et al. [17] and Niemenen et al. [10] have shown that DFT derived models of zeolites typically underestimate the dispersion/van der Waals interactions.

In this study the results from a series of calculations are reported that probe the influence of the QM cluster size and the extended framework treatment on the reaction energetics and structure formed during the *cis–trans* isomerisation of butene in H-ZSM-5 (Fig. 2). Seven different models have been employed; 3T, 5T and 10T DFT small cluster models, and to more effectively encode the extended framework of ZSM-5 3T:46T, 5T:46T, 10T:46T DFT:MM ONIOM models and a 46T DFT cluster model. While DFT functionals such as B3LYP have limitations, they have proved effective in predicting the isomerisation of 34 organic molecules. Tirado-Rives [18] report errors of 2.2 kcal/mol without corrections for dispersion and 1.9 kcal/mol with correction making them useful in this isomerisation study of butene. Subsequently, representative bond distances, angles, interaction distances and charges for the stationary points derived from each model are rigorously compared using principal components analysis (PCA) to quantitatively assess the structural differences that result from the different simulation conditions. This will provide useful insight into the strength and weakness of each of the different models when combined with an anlaysis of the reaction energetics.

Computational procedures

The 46 tetrahedra (nT) ONIOM model used here has been successfully applied to ZSM-5 on a number of previous occasions [7, 19–21]. The 46T representation was cut from the cross section of the straight channel and zigzag channel and the dangling bonds were saturated with hydrogen atoms as described elsewhere [7] (Fig. 1). This model has the advantage of being both computationally efficient and sufficiently precise based on reported agreement with experimental results. This is confirmed based on reports of Solans-Monfort et al. [9] who conclude that the long range effect in another zeolite, mordenite, does not extend far beyond the 38T region given the concordance between 38T ONIOM and DFT periodic models.

The ONIOM models consisted of the full 46T system where the inner region was varied from 3, 5 to 10T and treated using B3LYP/6–31G(d,p) method, with the remaining portion being simulated using the universal force field (UFF). During geometry optimisation only the substrate and the heavy atoms of the common 3T core (O, Si, Al) of the three different models were unrestricted. All stationary points were confirmed as such using frequency calculations. The three B3LYP/6–31G(d,p)//UFF models are henceforth referred to as 3T:46T, 5T:46T and 10T:46T. The single point energetics of the complete 46T system were reassessed at the B3LYP/6–31G(d,p) level using the optimised 10T:46T stationary points and are henceforth referred to as 46T for brevity.

For the purpose of comparison, 3T, 5T and 10T cluster models were also obtained at the B3LYP/6–31G(d,p) level.

Fig. 2 Stationary point on the potential energy surface associated with the conversion of *trans*-butene to *cis*-butene in ZSM-5. 3T model illustrated
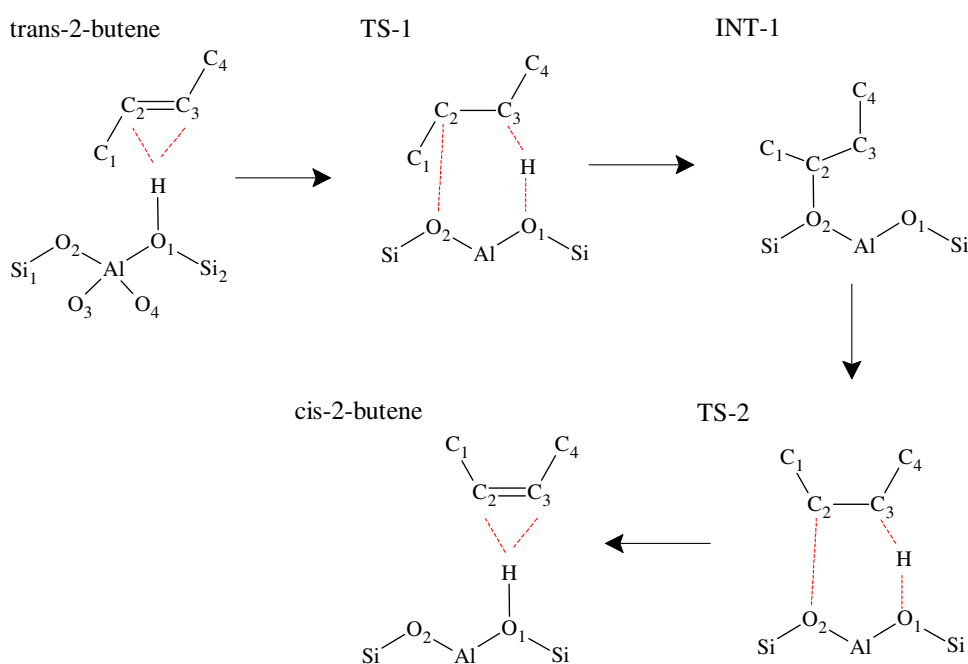
During geometry optimisation only the substrate and the heavy atoms of the common 3T core of the three models were free to optimise, with the dangling bonds being kept fixed to maintain the system in the same conformation as observed in ZSM-5.

Note, relaxation of the 3T cluster only during the calculations, with the remaining framework being fixed to their crystallographic positions, was deemed a necessary trade off between including the local effects of the zeolite structure accurately, in the quantum mechanical region, and the time required for the calculation to reach convergence. While clearly a limitation, this approach has proved itself useful in probing aspects of zeolite catalysis as exemplified by the work of Ferman et al. [22]. Additionally, the use of the 46T energies as a reference does not imply they are ideal, since it has already been noted the well-known limitations of DFT in describing van der Waals interactions. No experimental data is available for the substrates in this zeolite system so the 46T energies are used as a reference as they are the most accurate of the calculation performed here.

A PCA model was generated using 29 QM-derived geometric and electronic descriptors for the 30 different stationary points derived from the six different models. Descriptors consisted of the key bond distances and angles and the Mulliken charges on the heavy atoms of the system. The PCA model building process is the same as that reported elsewhere [2].

All the quantum mechanical calculations were performed using the Gaussian 03 program [23] and principal components analysis using SIMCA-P11.5 [24].

Results

The results obtained using the 3T, 5T and 10T cluster models are firstly discussed followed by a discussion of the more technically rigorous ONIOM results. The relative energetics associated with the *cis–trans* isomerisation reaction are reported in Table 1, and the optimised geometric parameters and the Mulliken charges found on the heavy atoms of the system are reported in Supplementary information (Tables S1–S6).

Cluster-based energetics

It is generally accepted that there are clear limitations to small cluster representations of zeolites. Nonetheless reports such as those from Boronat et al. [5] report that the cluster approach can realise comparable energies to the periodic approach if of a sufficient size such that it can account for the key steric, electronic and van der Waals effects of the zeolite framework, suggest this is not so clear-cut. This aspect is now discussed using the 3T, 5T, 10T and 46T results obtained here.

The correlation between the 3T, 5T, 10T and 46T energetics is strong indicating that larger clusters do not necessarily lead to different rank ordering of the stationary points. However, it is clear that the energies of the different transition states and intermediates increase as the size of the system decreases (Fig. 3a). For example the energy of the 3T model TS1 is 29.5 kcal/mol compared to 21.5 (5T), 19.4 kcal/mol (10T) and 15.6 kcal/mol for the 46T model. This effect is also observed for the intermediate and TS2

Table 1 *Cis–trans* isomerisation reaction energies expressed relative to the physisorbed zeolite complex for each respective level of theory

Energy/Kcal/Mol							
Model name	QM core size	Method	*trans*-2-butene	TS-1	Intermediate	TS-2	*cis*-2-butene
46T*	46T	Cluster	0	15.6	3.2	14.6	3
10T:46T	10T	ONIOM	0	21.7	10.3	21.1	0.9
10T	10T	Cluster	0	19.4	−1.6	21	2.6
5T:46T	5T	ONIOM	0	30.6	18.7	28	0.5
5T	5T	Cluster	0	21.5	2.8	23.1	1.5
3T:46T	3T	ONIOM	0	27.9	6.7	25.9	−0.6
3T	3T	Cluster	0	29.5	0	28.1	1.7

*46T B3LYP/6–31G(d,p) energies derived from a single point calculation on the 10T:46T optimised structures

indicating quite clearly that the larger the size of the QM cluster, the lower the energy barrier (Fig. 3a). This is in line with the reports elsewhere [5].

The 46T results are broadly in line with the 20T DFT representation of theta-1 used by Boronat et al. [25] for the 1-butene–*cis*-butene which had barrier of 18.9 kcal/mol. Additionally, the smaller cluster model results are also broadly in line with similar reports by Boronat et al. [26] and Li et al. [3], both reporting barriers of ~23.2 and 22.0 kcal/mol, respectively for 3T cluster models.

ONIOM-based energetics

The correlation between the 3T:46T, 5T:46T and 10T:46T is reasonably strong, again indicating that increasing the size of the QM region has little overall impact on rank ordering the 5 stationary points. As with the cluster models, the absolute energies of the different stationary points depend on the size of the QM system, however the trends are not as clear-cut (Fig. 3a). The 3T:46T and 5T:46T results are similar, but show higher energy transition states than the 10T:46T model, while the intermediates show the following trend 3T:46T < 10T:46T < 5T:46T. This discrepancy in the ordering when compared to the more simple gasphase calculations might be expected given reports elsewhere that ONIOM calculations do not treat the interaction between the layers correctly [27]. Nonetheless, the same reports state that QM:MM ONIOM geometries can realise energetics inline periodic models if single point energies of the complete system are obtained using DFT methods. This is analogous to the 46T model used here.

While the treatment of the electrostatics and van der Waals interactions appear non-ideal in this instance, it should be noted that Niemenen et al. [10] report that plane wave DFT calculations typically give adsorption energies too low due to the ineffective account of weak van der Waals interactions, with QM/MM embedded cluster methods offering a more reliable alternative. Jansang et al. [28] argue that transition state stabilisation is more strongly influenced by the electrostatic contribution compared to the van der Waals effects based on their ONIOM calculations.

ONIOM vs. cluster-based energetics

The effect of the extended MM region over and above the gasphase cluster can be displayed graphically in Fig. 3b, where the nT cluster energies are plotted against the equivalent nT ONIOM energies. It is apparent that the MM regions do not significantly alter the energies of the transition states or minima obtained in the ONIOM calculations given the near 1 to 1. The only outliers between the ONIOM and cluster calculations are the intermediates where the presence of the extended framework leads to significant destabilisation. This destabilisation is probably not as pronounced as these calculations would suggest, since when a single point energy is performed on the whole 46T system, the intermediate energy lies between that of the ONIOM and cluster models values.

In an effort to account for the energy difference between the 46T and 10T:46T model, the former being obtained from the optimised coordinate of the latter, we analysed the QM-derived electronics and geometric parameters available. Plotting the absolute charge on the heavy atoms of the zeolite, a measure of the dispersion of the electron density over it and the substrate, one finds that the difference in energy is almost completely a result of the electrostatic stabilisation (Fig. 3c). This is inline with reports from Jansang et al. [28].

Structural differences between models

PCA is a method for reducing the amount of data to be analysed by exploiting the correlated nature of the variables and is frequently used in the field of Cheminformatics [29]. By taking linear combinations of the key correlated variables, the majority of the variance of the original data can be described by a smaller number of orthogonal latent variable or components. These can then be used to assess
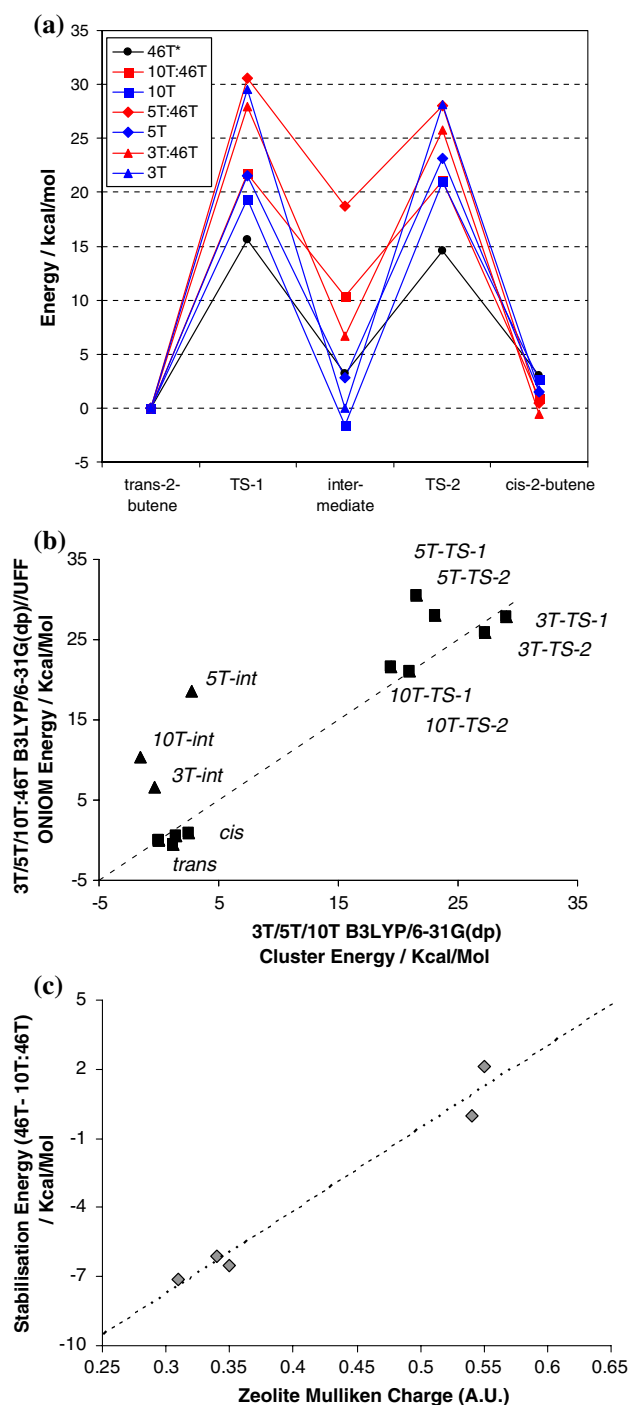
Fig. 3 (**a**) Energy profile for the 3T, 5T or 10T ONIOM and cluster energies (**b**) plot of the ONIOM model energies versus the corresponding gasphase energies. The line of unity is denoted by the black dot-dash line. (**c**) Plot of the energy difference between the 46T and 10T:46T models versus the Mulliken charge on the zeolite heavy atoms

the correlated nature of the changes moving between the different stationary points on the reaction coordinate. For a more detailed description of the method see reference [2].

The PCA model fits four orthogonal components, describing approximately 84% of the total variance in the 29 descriptors derived from 30 observations. Component one of the PCA model describes 46% of the variance, followed by component two accounting for 16%, component three, 13% and finally, component four, 9%. This means the corresponding scores and loadings plots offer a real advantage in the interpretation of the structural and electronic data (Fig. 4).

Component one consists of the structural factors that separate *cis* and *trans*-butene from the transition states and intermediate (Fig. 4a). The descriptors that give rise to this separation on component one are those with the largest loading, those with a positive sign increasing in magnitude going from left to right and those with a negative sign decreasing. This component understandably therefore describes the structural changes associated with the migration of the acidic proton (Hz) from the zeolite to the substrate, the resulting increase in the O1–Hz bonds and the decrease in the rC2–O2 and rC3–Hz bond (Fig. 4b). Along with these changes, it is clear from the loadings plot that the net negative charge on the substrate decreases and on the zeolite it increases. Component two describes the structural factors that separate the transition states from minima and from an analysis of the loadings plot (Fig. 4b) it is found that this corresponds primarily to the decrease in the rC1–C2 bond in the minima and the rC3–O1 bond between the zeolite and the substrate.

Component one and two describe 62% of the total variance, accounting for the differences between the different stationary points and do not show any dependence on the different methodologies. In contrast, components three and four, accounting for an additional 22% of variation describes the structural factors that separate the models with different sized QM cores (component three) and the ONIOM from the cluster models (component four). The fact that component three accounts for 13% of the variation and component four, 9%, suggests the size of the QM cluster has a larger impact on the structures of the stationary points compared to the presence of the MM framework. Furthermore, the fact that the 10T and 5T results are found close together on component three suggests that the structural implications of changing between the two is much smaller than going to a 3T model. This collectively suggests that a 5T:46T ONIOM model employing a full 46T single point represents a reasonable compromise between optimum speed and energetics.

The main difference of increasing the size of the QM core is that the net negative charge on the zeolite on average decreases and the net negative charge on the Al atom increases. Additionally moving to larger QM cores sees a decrease in the rO1-Si2, rAl-O1, rO2-Si1 distances on average. The structural factors leading to the separation of the ONIOM and cluster calculations are also the Al
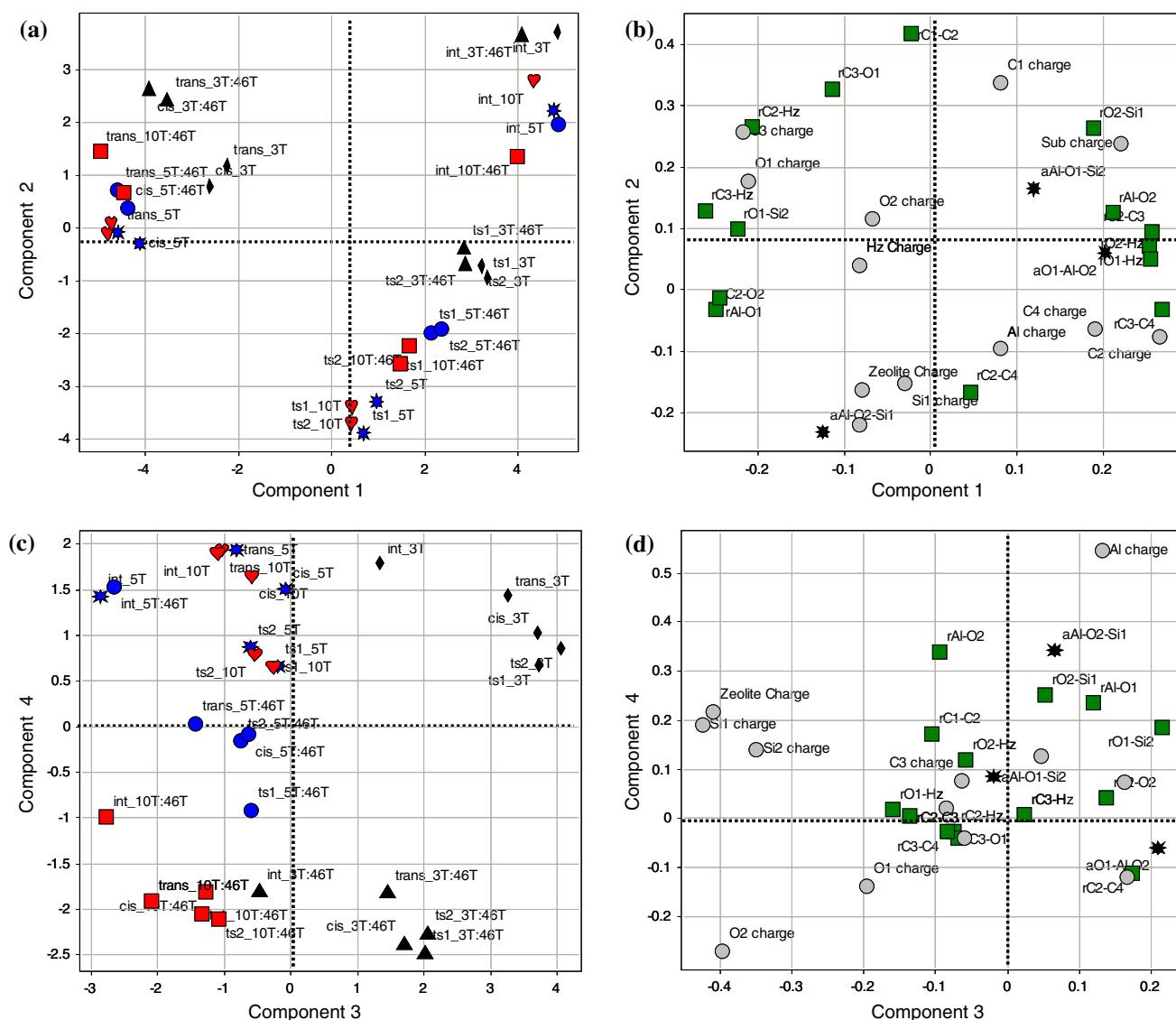
Fig. 4 Scores (**a**, **c**) and loading (**b**, **d**) for components 1–2 (top) and 3–4 (bottom). Total number of observations = 30, descriptors = 29. On the scores plots ONIOM models are denoted red and gasphase models blue while individual models are denoted as follows; 3T = diamond, 5T = star, 10T = heart, 3T:46T = triangle, 5T:46T = circle, 10T:46T = square. On the loading plots, distances are denoted using squares, Mulliken charges using circles and angles using stars

charge, which is less positive, and the O2 charge which is more negative on average in the ONIOM calculations. Other differences include the rAl-O1 and rAl-O2 distances which are longer in the gasphase models.

It should be noted that PCA model here does not account for 16% of the variation in the structural parameters. Adding additional components is possible however it is not possible to ascribe these to any single factor.

Conclusions

In this study the results from a series of calculations on *cis–trans* isomerisation are reported that probe the influence of the QM cluster size and the extended framework treatment in ONIOM calculations. The results show that irrespective of the exact QM cluster size, relatively small gasphase clusters are limited due to the neglect of the extended framework. ONIOM methods represent a more effective method to account for structural constraints of the zeolite and this results in energetics closer to larger QM models. Additionally, these simulations suggest the energetics obtained using the ONIOM QM:MM method are not that reliable, but this deficiency can be rectified using single point energy calculations.

The structural and electronic implications of using the different zeolite models have been rigorously assessed using the multivariate statistical method principal components

analysis (PCA). These results clearly show the discrepancies between simulations that encode and do not encode the structural features of the zeolite framework. The key advantage of the QM:MM scheme is to efficiently encode the structural constraint imposed by the local framework and leads to structurally different results to gasphase cluster calculations.

We find the 5T:46T QM:MM method is an effective way to encode the steric and electrostatic effect of the local environment in a computationally efficient manner.

References

1. Davidova M, Nachtigallova D, Nachtigall P (2004) J Phys Chem B 108:13674–13682
2. Tantanak D, Gleeson MP, Limtrakul J (2005) J Chem Inf Mod 45:1303–1312
3. Li HY, Pu M, Liu KH, Zhang BF, Chen BH (2005) Chem Phys Lett 404:384–388
4. Rattanasumrit A, Ruangpornvisuti V (2005) J Mol Catal A:Chem 239:68–75
5. Boronat M, Zicovich-Wilson CM, Viruela P, Corma A (2001) J Phys Chem B 105:11169–11177
6. Gleeson D, Limtrakul J (2007) J Mol Struct (THEOCHEM) 824:23–31
7. Namuangruk S, Tantanak D, Limtrakul J (2006) J Mol Catal A:Chem 256:113–121
8. Jansang B, Nanok T, Limtrakul J (2007) J Mol Catal A:Chem 264:26433–26439
9. Solans-Monfort X, Sodupe M, Branchadell V, Sauer J, Orlo R, Ugliengo P (2005) J Phys Chem B 109:3539–3545
10. Nieminen V, Sierka M, Murzin DY, Sauer J (2005) J Catal 231:393–404
11. Shiota Y, Suzuki K, Yoshizawa K (2006) Organometallics 25:3118–3123
12. Shor EAI, Shor AM, Nasluzov VA, Vayssilov GN, Rosch N (2005) J Chem Theory Comput 1:459–471
13. Clark LA, Sierka M, Sauer J (2004) J Am Chem Soc 126:936–947
14. Rozanska XX, Barbosa LAMM, van Santen RA (2005) J Phys Chem B 109:2203–2211
15. Brandle M, Sauer J, Dovesi R, Harrison NM (1998) J Chem Phys 109:10379–10389
16. Brandle M, Sauer J (1997) J Mol Catal Chemical A 119:19–33
17. Tuma C, Sauer J (2006) Phys Chem Chem Phys 8:3955–3965
18. Tirado-Rives J, Jorgensen WL (2008) J Chem Theory Comput 4:297–306
19. Namuangruk S, Pantu P, Limtrakul J (2005) J Chem Phys Chem 6:1333
20. Namuangruk S, Khongpracha P, Pantu P, Limtrakul J (2006) J Phys Chem B 110:25950–25957
21. Jungsuttiwong S, Limtrakul J, Truong TN (2005) J Phys Chem B 109:13342–13351
22. Fermann JT, Moniz T, Kiowski O, McIntire TJ, Auerbach SM, Vreven T, Frisch MJ (2005) J Chem Theory Comput 1:1232–1239
23. Gaussian 03, Revision C02, Frisch MJ, Trucks, GW, Schlegel HB, Scuseria GE, Robb MA, Cheeseman JR, Montgomery JA, Vreven T, Kudin KN, Burant JC, Millam JM, Iyengar SS, Tomasi J, Barone V, Mennucci B, Cossi M, Scalmani G, Rega N, Petersson GA, Nakatsuji H, Hada M, Ehara M, Toyota K, Fukuda R, Hasegawa J, Ishida M, Nakajima T, Honda Y, Kitao O, Nakai H, Klene M, Li X, Knox JE, Hratchian HP, Cross JB, Bakken V, Adamo C, Jaramillo J, Gomperts R, Stratmann RE, Yazyev O, Austin AJ, Cammi R, Pomelli C, Ochterski JW, Ayala PY, Morokuma K, Voth GA, Salvador P, Dannenberg JJ, Zakrzewski VG, Dapprich S, Daniels AD, Strain MC, Farkas O, Malick DK, Rabuck AD, Raghavachari K, Foresman JB, Ortiz JV, Cui Q, Baboul AG, Clifford S, Cioslowski J, Stefanov BB, Liu G, Liashenko A, Piskorz, P, Komaromi I, Martin RL, Fox DJ, Keith T, Al-Laham MA, Peng CY, Nanayakkara A, Challacombe, M, Gill PMW, Johnson B, Chen W, Wong MW, Gonzalez C, Pople J A, Gaussian, Inc, Wallingford CT, 2004
24. SIMCA-P 10, Umetrics, Tvistevägen 48, Box 7960, SE-907 19 Umeå, Sweden. www.umetrics.com
25. Boronat M, Viruela P, Corma A (2001) Phys Chem Chem Phys 3:3235–3339
26. Boronat M, Viruela P, Corma A (1998) J Phys Chem A 102:982–989
27. Boronat M, Viruela P, Corma A (2004) J Am Chem Soc 126:3300–3309
28. Jansang B, Nanok T, Limtrakul J (2006) J Phys Chem B 110:12626–12631
29. Gasteiger J (2003) Chemoinformatics: a textbook Wiley VCH